Effect of Divalent Cocations on the Location and Coordination of Cu^{2+} in X Zeolites: Electron Spin Resonance and Electron Spin Echo Modulation Spectroscopic Studies of Cu-CdX Zeolite

M. Narayana and Larry Kevan*

Department of Chemistry, University of Houston, Houston, Texas 77004

Received February 19, 1985

Electron spin resonance (ESR) and electron spin echo modulation (ESEM) spectroscopic techniques have been used to study the site location and environment of Cu^{2+} in fully cadmium exchanged X zeolite. In fresh and rehydrated samples the ESR studies indicate Cu^{2+} to be present as a trigonal-bipyramidal complex. Analysis of the deuterium modulation in the ESEM spectra indicates the interaction of Cu^{2+} with two close deuteriums and four slightly farther deuteriums. The copper species is proposed to be $Cu(O_z)_3(OH)_2$, with the Cu^{2+} located in a six-ring window at site SII between the α- and β-cages of the zeolite, similar to the copper species observed in Cu-CaX zeolite. The similarities and differences between Cu-CdX and Cu-CaX zeolites are discussed.

Introduction

The structure and catalytic properties of cupric ion loaded zeolites have been studied by various techniques.[1-4] Electron spin resonance (ESR) has been extensively used[5,6] to characterize the behavior of Cu^{2+} as the zeolite is subjected to various treatments. However, in many cases the ESR spectra cannot be interpreted to obtain unequivocal short-range order around the paramagnetic species. Recent work has shown[7-11] that electron spin echo modulation (ESEM) spectroscopy is a powerful technique to determine weak dipolar and quadrupolar interactions between the paramagnetic species and the surrounding magnetic nuclei even in powders and disordered systems. These interactions cannot be measured by conventional ESR methods. We have shown[11-14] recently that the location and coordination of Cu^{2+} in X zeolites is very sensitively dependent on the major cocation. Cu^{2+} was found to occupy relatively inaccessible sodalite or β-cage sites in NaX[12] while it formed hexaaquo complexes in the large cages of the zeolite in TlX.[13] Our ESR and ESEM studies of Cu^{2+} in CaX[15] indicate the formation of a new trigonal-bipyramidal complex in the six-ring window between the α- and β-cages in the zeolite structure. To extend these studies of divalent cation effects we have examined the ESR and ESEM of Cu^{2+} in CdX zeolite.

Experimental Section

Linde 13X (NaX) was washed with 0.1 M sodium chloride solutions to remove impurity Fe^{3+}. Then the zeolite was ion exchanged with 0.1 M cadmium perchlorate solutions at 353 K to obtain CdX zeolite. Complete exchange of Cd^{2+} was confirmed by elemental analysis. About 0.3% of Cd^{2+} was exchanged with Cu^{2+} using 0.1 mM $Cu(NO_3)_2$ solutions at room temperature with the pH of the solution adjusted to 4.5-5.0 using nitric acid. The filtered zeolite was washed 4 times with hot multiply distilled water to remove any physically present $Cu(H_2O)_6^{2+}$ species. Then the zeolite was air dried at room temperature (humidity, 60%). Samples of Cu-CdX from such preparations are referred to as fresh samples. Samples for ESR and ESEM studies were prepared by loading the zeolite powder into 3-mm-o.d. Suprasil quartz tubes. The following treatments were carried out for various experiments: (1) For studying the changes in ESR spectra as a function of the temperature of dehydration, the zeolite in 3-mm o.d. quartz tubes was attached to a vacuum line and dehydrated at 293, 323, 373, 473, or 673 K to a residual pressure of 2×10^{-6} torr. Samples dehydrated at 473 or 673 K were oxidized at that temperature with 500 torr of O_2 (99.99%, Linde) for 3 h, evacuated for 6 h, and then sealed. (2) Samples of Cu-CdX for studies of deuterium modulation in the ESEM experiments were prepared (a) by soaking the fresh sample in D_2O for 24 h, evacuating at 293 K for 12 h, and sealing and (b) by evacuation of the oxidized sample at 583 K, cooling the sample to ambient temperature, exposure to D_2O vapor for 12 h, and sealing. (3) Some dehydrated, oxidized samples were exposed to methanol vapor for 3 h at room temperature, evacuated for 20 min, and sealed with the sample tube under liquid nitrogen.

The ESR spectra at room temperature and 77 K were recorded with a modified Varian E-4 spectrometer and the ESEM spectra were recorded at 4.2 K with a homebuilt spectrometer.[15]

Results

Figure 1 shows the ESR spectra at 77 K of Cu^{2+} in Cu-CdX zeolite after various treatments. Only one Cu^{2+} species was observed in all fresh samples of Cu-CdX (Figure 1a). It has the unusual feature of "reversed" g values ($g_\parallel < g_\perp$) and well-resolved hyperfine features ($^{63,65}Cu$, $I = {}^3/_2$) even at room temperature, which is indicative of a long spin-lattice relaxation time. This copper species will be referred to as Cu(A). The spectral features of Cu(A) do not change on prolonged evacuation of the sample at 293 or 323 K. On raising the evacuation tem-

(1) Richardson, J. T. *J. Catal.* **1967**, *9*, 182.
(2) Dickson, B. L.; Rees, L. V. C. *J. Chem. Soc., Faraday Trans. 1* **1974**, *70*, 2038.
(3) Peigneur, P.; Lunsford, J. H.; De Wilde, W.; Schoonheydt, R. A. *J. Phys. Chem.* **1977**, *81*, 1179.
(4) Ben Taarit, Y.; Che, M. In "Catalysis by Zeolites"; Imelik, B., Naccache, C., Ben Taarit, Y., Vedrine, J. C., Couduvier, G., Praliaud, H., Eds.; Elsevier: New York, 1980; pp 167-193.
(5) Conesa, J. C.; Soria, J. *J. Chem. Soc. Faraday Trans. 1* **1979**, *75*, 406.
(6) (a) Flentge, D. R.; Lunsford, J. H.; Jacobs, P. A.; Utterhoeven, J. B. *J. Phys. Chem.* **1975**, *79*, 354. (b) Herman, R. G.; Flentge, D. R. *J. Phys. Chem.* **1978**, *82*, 720. (c) Herman, R. G. *Inorg. Chem.* **1979**, *18*, 995.
(7) Mims, W. B.; Peisach, J.; Davis, J. L. *J. Chem. Phys.* **1977**, *66*, 5536.
(8) Ichikawa, T.; Kevan, L.; Bowman, M. K.; Dikanov, S. A.; Tsvetkov, Yu. D. *J. Chem. Phys.* **1979**, *71*, 1167.
(9) Kevan, L. In "Time Domain Electron Spin Resonance"; Kevan, L., Schwartz, R. N., Eds.; Wiley-Interscience: New York, 1979; Chapter 8.
(10) (a) Mercks, R. P. J.; de Beer, R. *J. Magn. Reson.* **1980**, *37*, 305. (b) Mercks, R. P. J.; de Beer, R. *J. Phys. Chem.* **1979**, *83*, 3319.
(11) Kevan, L.; Narayana, M. In "Intrazeolite Chemistry"; Stucky, G. D., Dwyer, F. G., Eds.; American Chemical Society: Washington, DC, 1983; ACS Symp. Ser. No. 218, pp 284-299.
(12) Ichikawa, T.; Kevan, L. *J. Am. Chem. Soc.* **1983**, *105*, 402.
(13) Narayana, M.; Kevan, L. In "Proceedings of the Sixth International Zeolite Conference"; Bissio, A.; Olsen, D. H., Eds.; Butterworth Scientific: London, 1984.
(14) Narayana, M.; Kevan, L. *J. Chem. Phys.* **1983**, *78*, 3573.
(15) Ichikawa, T.; Kevan, L.; Narayana, P. A. *J. Phys. Chem.* **1978**, *83*, 3378.

0743-7463/85/2401-0553$01.50/0

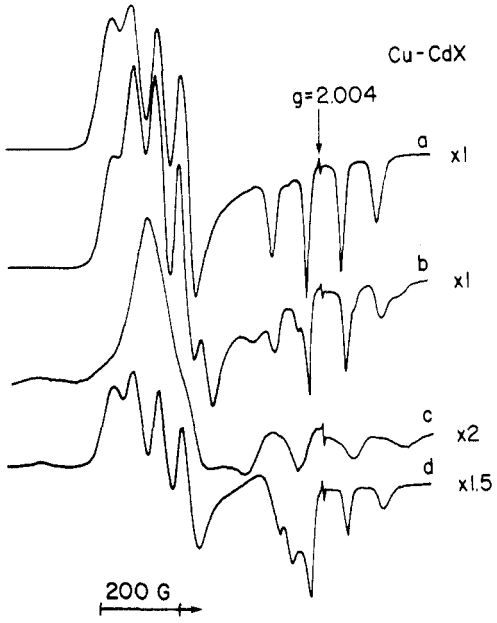

Figure 1. ESR spectra of Cu^{2+} in Cu–CdX zeolite at 77 K after various treatments to the zeolite: (a) sample evacuated to 10^{-5} torr at 323 K for 24 h; (b) sample evacuated to 10^{-5} torr at 373 K for 12 h; (c) sample evacuated to 10^{-5} torr at 393 K for 12 h; (d) sample evacuated to 10^{-5} torr at 583 K for 12 h, oxidized at the same temperature with 500 torr O_2 for 3 h, evacuated again for 6 h at the same temperature, cooled to ambient temperature, and exposed to D_2O vapor for 12 h. The sharp line seen at g = 2.004 in all the spectra is due to a color center in the ESR Dewar.

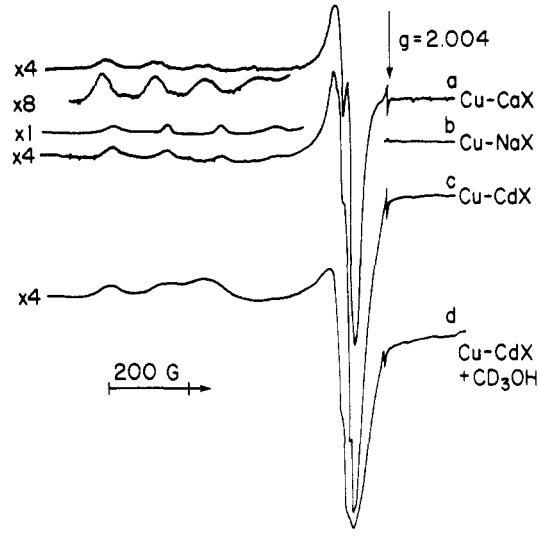

Figure 2. ESR spectra of Cu^{2+} in various X zeolites, dehydrated at 673 K for 16 h, oxidized at the same temperature with 500 torr of O_2 for 3 h, and evacuated to 10^{-5} torr at the same temperature for 6 h: (a) Cu–CaX; (b) Cu–NaX; (c) Cu–CdX; (d) Cu–CdX exposed to CD_3OH vapor for 2 h at 293 K. The $A_\perp$ hyperfine components of Cu–NaX were deleted for clarity.

perature to 373 K, a second Cu^{2+} species Cu(A′) is seen (Figure 1b), also with reversed g values. Exposure of the sample to either water vapor or air for about 3 h quickly restores Cu(A) as the single ESR active species. If the zeolite is dehydrated at 393–423 K, Cu(A) completely disappears, Cu(A′) becomes the dominant species, and a weak new species with "normal" g values ($g_\parallel > g_\perp$) appears with only its low-field hyperfine line being clearly resolved, as shown in Figure 1c. Once again Cu(A) is regenerated as the sole species on exposing such a dehydrated sample to water vapor or air. However, if the dehydration/evacuation is done at temperatures higher than 453 K,

Table I. Spin-Hamiltonian Parameters of Cu^{2+} in X Zeolites

zeolite	copper species	hydration status[a]	$g_\parallel$[b]	$g_\perp$[b]	$A_\parallel$[c]	$A_\perp$[c]
Cu–CdX	Cu(A)	1	1.995	2.299	85	64
	Cu(A)	2	1.995	2.300	84	64
	Cu(A′)		2.002		115	
	Cu(A′)	3	2.002	2.254	127	
	Cu(B)	4	2.360	2.070	148	>15
	Cu(A)	5	1.995	2.300	84	65
Cu–CaX		1	2.001	2.300	93	59
		2		no change		
		3		no change		
		4	2.379	2.071	133	>15
		5	2.002	2.300	94	58
Cu–NaX		4	2.363	2.070	138	17

[a] The hydration status numbers have the following meanings: 1, freshly prepared, hydrated samles; 2, dehydrated at 373 K for 12 h; 3, dehydrated at 400 K for 18 h; 4, dehydrated at 673 K and oxidized; 5, dehydrated at 400 K, cooled to room temperature, and exposed to water vapor for 3 h to give a rehydrated sample. [b] The errors in the g-value measurements are estimated as ±0.003. [c] The units of $A_\parallel$ and $A_\perp$ are in 10^{-4} cm^{-1} with an estimated measuring error of $\pm 2 \times 10^{-4}$ cm^{-1}.

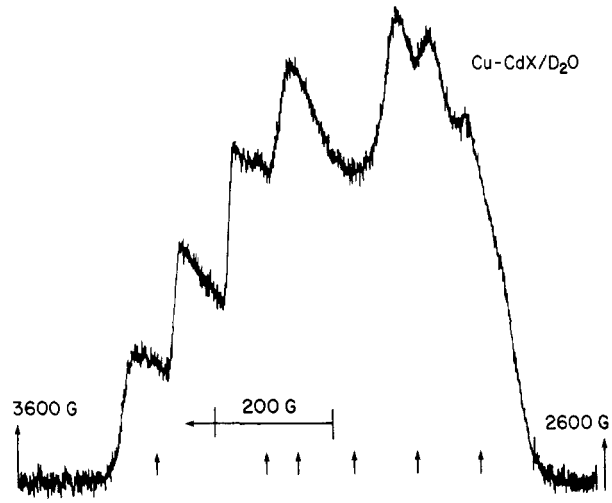

Figure 3. Electron spin echo induced ESR spectrum of Cu^{2+} in Cu–CdX/H_2O at 4.2 K. Arrows indicate the magnetic field positions at which ESEM was measured. The interpulse time was set at 0.300 μs.

Cu(A′) also disappears completely and only the species with normal g values, referred to as Cu(B), is seen. Such a spectrum in Cu–CdX dehydrated at 673 K is shown in Figure 2 along with the ESR spectra of Cu–CaX and Cu–NaX also dehydrated and oxidized at 673 K. After oxidation at 673 K, exposure of Cu–CdX zeolite to water vapor restores Cu(A) as the dominant Cu^{2+} species, but a small amount of Cu(B) remains (Figure 1d). As the temperature of dehydration increases, the percentage of Cu(B) that remains after rehydration increases. Shown in Figure 2d is the ESR spectrum obtained after adsorption of methanol on a Cu–CdX sample dehydrated and oxidized at 673 K. A very weak spectrum with reversed g values is seen to be superposed on this spectrum. The ESR parameters of the copper species are summarized in Table I.

Figure 3 shows the ESR spectrum induced by electron spin echoes. It is obtained by scanning the magnetic field while keeping the interpulse time in a two-pulse experiment[9] fixed. In a three-pulse experiment,[9] by judicious choice of the time interval τ between the first two pulses, it is possible to suppress one modulation frequency. When the zeolite is deuterated, τ is chosen so as to suppress the

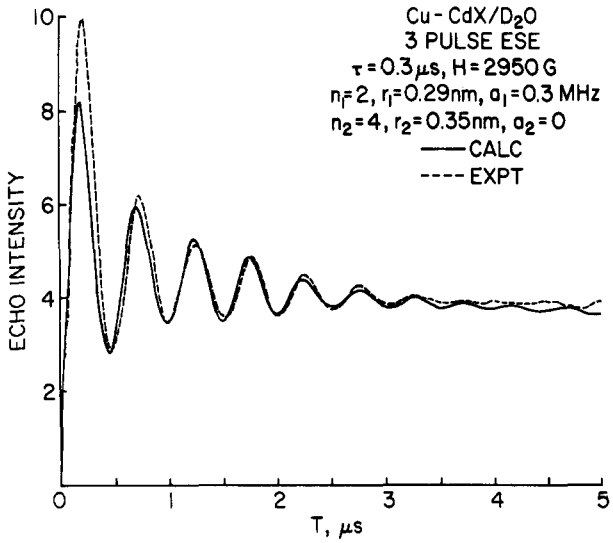

Figure 4. Calculated and experimental deuterium modulation in the three-pulse ESEM spectra of Cu–CdX prepared as in Figure 1d. The best fit was obtained with a two-shell model.[9] The decay function was $\exp(2.30 - 0.07T + 0.005T^2)$.

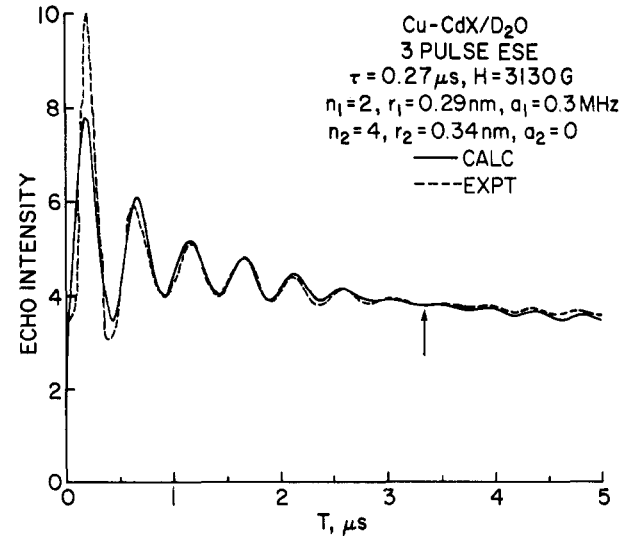

Figure 5. Calculated and experimental deuterium modulation in the three-pulse ESEM spectra of Cu–CdX prepared by soaking a fresh sample in D_2O for 24 h and then evacuating at room temperature for 12 h. The parameters for the best fit are in very good agreement with those in Figure 4. The decay function used was $\exp(2.52 - 0.11T + 0.008T^2)$. The arrow indicates the time point at which phase reversal occurs in the experimental data which is reproduced in the simulation.

modulation from the aluminum nuclei of the zeolite framework, thus facilitating the selective detection and analysis of deuterium modulation. The three-pulse ESEM spectra thus obtained at two different magnetic field settings are shown in Figures 4 and 5. These and other three-pulse ESEM spectra were analyzed by methods described earlier[8,9,16] and indicate that Cu^{2+} in CdX interacts with two types of deuterons, two at 0.29 nm with 0.3-MHz isotropic hyperfine coupling and four at 0.34 nm with zero isotropic hyperfine coupling. The distance is determined to ±0.01 nm and the isotropic hyperfine coupling is determined to ±10% by comparison of simulated and experimental ESEM spectra.

A fairly good estimate of the nuclear quadrupole coupling and isotropic hyperfine coupling and information about the inequivalence, if any, of the interacting nuclei are usually obtained by fast Fourier transformation (FFT) of the time domain ESEM data into the frequency domain.[16,17] Figure 6 shows the FFT spectrum of a three-pulse ESEM spectrum obtained for Cu–CdX zeolite with adsorbed D_2O. The FFT spectra of two-pulse ESEM spectra in fresh samples (i.e., hydrated) of Cu–CdX at two different magnetic field settings are shown in Figure 7. The various frequencies seen in Figures 6 and 7 and in other FFT spectra are tabulated in Table II. Also given in the table are the Zeeman frequencies of ^{27}Al, ^{2}D, and ^{1}H at the various magnetic field settings.

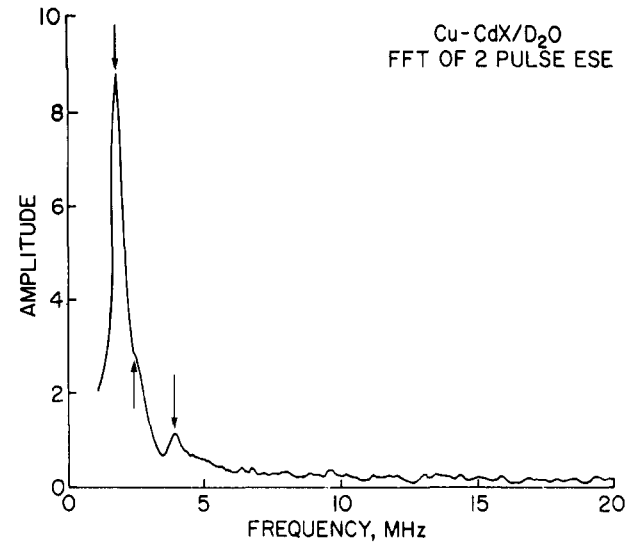

Figure 6. Fast Fourier transform of the three-pulse ESEM spectrum of Cu–CdX/D_2O. The arrows indicate frequencies of 1.86, 2.55, and 3.92 MHz, respectively. The ESEM spectrum was recorded at H = 3100 G with τ = 0.27 μs. The taper parameter used in the transformation was 0.1.

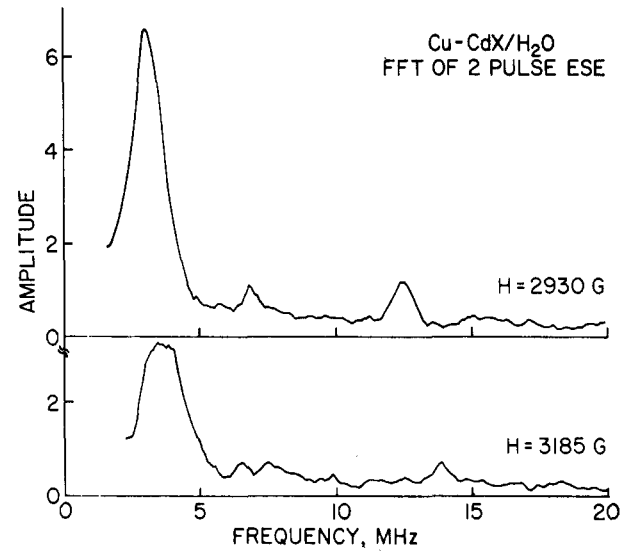

Figure 7. Fast Fourier transforms of the two-pulse ESEM spectra of fresh samples of Cu–CdX at two different values of the magnetic field: (a) H = 2930 G and (b) H = 3185 G. The taper parameter used in the transformation was 0.1.

Discussion

Zeolite X is composed of alternating AlO_2 and SiO_2 tetrahedra with a Si/Al ratio of 1.25. These units are linked to form truncated octahedra called sodalite cages or β-cages. Tetrahedral linkages of several of these sodalite cages through a double-six-ring unit called a hexagonal

(16) Narayana, P. A.; Kevan, L. *Magn. Reson. Rev.* **1983**, *7*, 239.
(17) Van Ormondt, D.; Nederveen, K. *Chem. Phys. Lett.* **1981**, *82*, 443.

Table II. Superhyperfine Frequencies in Cu–CdX Zeolite

nucleus	magnetic field, G	Larmor frequency, MHz	obsd frequency,[b] MHz
^{27}Al	2930	3.25	3.25
		6.50[a]	6.90
	3185	3.53	3.33, 4.04
		7.06[a]	6.60, 7.80
^{1}H	2930	12.48	12.60
	3185	13.54	14.19
^{2}D	2930	1.91	1.85, 2.45, 3.90[c]
		3.83[a]	3.66
	2950	1.93	1.85, 2.43, 3.95[c]
	3100	2.03	1.88, 2.55, 3.92[c]
	3130	2.05	2.00, 2.60
		4.09	4.13

[a] Second harmonic of the Larmor frequency. [b] Measuring accuracy is ±0.05 MHz. [c] Clearly seen only in three-pulse experiments (see Figure 6) with the magnetic field set at or below 3100 G.

prism completes the unit cell of X zeolite. Such an arrangement results in larger cages called α-cages. Because of the excess negative charge present on the AlO_2 units, compensating cations are present to balance the charge in the zeolite framework. Some of the specific sites occupied by these charge compensating cations have been identified by X-ray crystallographic studies.[18] SI is the site in the middle of the hexagonal prism and SI′ is the displaced site into the β-cage. SII is the site in the center of the six-ring window between the α- and β-cages while SII′ and SII* represent sites displaced from this window into the β- and α-cages, respectively.

The appearance of a Cu^{2+} with reversed g values as the sole species even when the zeolite is fully hydrated is highly unusual. With the exception of Cu–CaX zeolite, in all other fully hydrated A, X, and Y zeolites Cu^{2+} is observed with normal g values. Herman[6] observed a *partial* conversion of Cu^{2+} in NaA and NaY zeolites into a species with reversed g values upon evacuation for prolonged intervals at various temperatures. We have also observed[11] a similar *partial* conversion of Cu^{2+} in several A and X zeolites on vacuum treatment at room temperature or by drying in air at 383 K. Only in Cu–CaX have we observed a Cu^{2+} with $g_{\parallel} < g_{\perp}$ even when the zeolite is fully hydrated. Thus Cu–CdX seems to be very similar to the calcium exchanged zeolite. Here it is noted that in our preliminary experiments with other divalent ion exchanged X zeolites such as BeX, MgX, BaX, and ZnX we did *not* observe the reversed g value spectrum for Cu^{2+} in the fresh, hydrated samples. Thus Cu^{2+} in CdX and CaX seems to behave uniquely.

However, the behavior of Cu^{2+} in Cu–CaX and Cu–CdX zeolites was found to be rather different as the dehydration temperature was increased from room temperature to 453 K. In Cu–CaX the spectral parameters do not change significantly as the dehydration temperature is increased from 293 to 400 K, while in Cu–CdX they do change significantly (see Table I) and a second Cu^{2+} species, Cu(A′) with different parameters, is seen. Also in fully dehydrated Cu–CaX and Cu–CdX the ESR parameters are distinctly different indicating that Cu^{2+} might move to two different sites, during dehydration, in these two zeolites.

The reversal of the order of g values occurs[19] for Cu^{2+} when the unpaired spin has a $|3z^2 - r^2\rangle$ state as the predominant part of the ground-state wavefunction. The coordination geometries leading to such a ground state are:[20] (a) trigonally compressed tetrahedron, (b) tetragonally compressed octahedron, (c) cis distorted octahedron, (d) compressed square pyramidal and (e) trigonal bipyramidal configuration. We have shown[14] that in hydrated Cu-CaX the most likely configuration for Cu^{2+} is trigonal bipyramidal geometry with the Cu^{2+} at site SII interacting with three zeolitic oxygens in the six ring window and with two hydroxyl groups, one in the β-cage and the other in the α-cage, to complete the fivefold coordination.

It seems likely that Cu^{2+} in fresh hydrated or in rehydrated samples of Cu–CdX exists in a similar configuration. While the first interacting shell of deuteriums in Cu–CdX, deduced from ESEM analysis, is identical in number and distance with those in Cu–CaX, the total number of interacting deuteriums in Cu–CdX is twice as many. In Cu–CaX, the second-shell deuteriums were proposed to be deuteroxyl groups possibly connected to calcium ions at SI′ sites since the ESEM spectra of fresh, hydrated samples and the ones of samples dehydrated at 373 K showed identical ESR and ESEM spectra. Such is not the case in Cu–CdX in which the ESR spectrum resolves into that of two Cu^{2+} species upon dehydration at 393 K. Thus the second shell deuterons in Cu–CdX are more likely to be water molecules in the α-cage. Unfortunately, due to the short phase memory times in the dehydrated samples, meaningful analyses of the ESEM spectra could not be carried out.

From the deuterium frequencies observed in the FFT spectra of Cu–CdX (Figure 6 and Table II) it is clear that there are at least two types of deuteriums interacting with Cu^{2+}, one close to its Lamor frequency which is indicative of zero contact or isotropic hyperfine coupling with the unpaired electron spin and the other with some delocalization of the unpaired spin. This is in good agreement with our time domain simulations. Because of the lack of deconvolution algorithms, it is difficult to estimate the isotropic hyperfine coupling accurately from these spectra, but it seems to be of the order of 0.4–0.8 MHz. The best fit obtained for the time domain data was with 0.3 MHz. In principle the resolution in the FFT spectra of the ESEM data could be improved by mathematical manipulations suggested by Van Ormondt and Nederveen,[17] but their treatments generally require experimental data over longer time periods than was possible to obtain in our samples.

The aluminum modulation from the framework aluminum nuclei in the fresh, hydrated samples could not be quantitatively analyzed in the time domain simulations since the expressions normally used for the analysis ignore the nuclear quadrupole interaction or include it with an inadequate approximation for large quadrupole interactions. Some trial simulations obtained with a second-order perturbation theory treatment of the quadrupole interaction indicate that the quadrupole interaction of aluminum nuclei is less than 2.0 MHz in the Cu–CdX/H_2O samples. From Table II and Figure 7b it is seen that the aluminum nuclei in the six-ring window are interacting quite strongly with Cu^{2+} as indicated by the significant difference from the free precession values for a magnetic field setting of 3185 G, which is close to the $g_{\parallel}$ direction.

Finally, it is important to comment on possible reasons for Cu^{2+} to occur in the otherwise unusual trigonal-bipyramidal coordination in hydrated CdX zeolite. In our previous work we have shown that Cu^{2+} prefers the SI sites in the hexagonal prisms in NaX zeolite while it forms a

(18) Smith, J. V. In "Zeolite Chemistry and Catalysis"; Rabo, J. A., Ed.; American Chemical Society: Washington, DC, 1976; Chapter 1.
(19) Abragam, A.; Bleaney, B. "Electron Paramagnetic Resonance of Transition Ions"; Oxford: London, 1970; p 456.
(20) (a) Hathaway, B. J.; Billing, D. E. *Coord. Chem. Rev.* **1970**, *5*, 143. (b) Gibson, J. F. In "Electron Spin Resonance"; Norman, R. O. C., Ed.; The Chemical Society: London, 1970; Vol. 3, p 116.

triaquo complex at SII* in KX zeolite and a hexaaquo complex in the α-cages in TlX zeolite.[12,13] In the last case, the high affinity of Tl^+ for the SI′ and SII sites was thought to be a prime factor resulting in Cu^{2+} forming hexaaquo complexes in the α-cage. There is no crystal structure data available for CdX zeolite. From the close similarities of Cu^{2+} behavior in CaX and CdX we conclude that in CdX, Cd^{2+} is most probably in SI′ sites thus preventing Cu^{2+} from occupying the SI′ or SI sites. Thus Cu^{2+} ends up in SII sites. The decrease in the $g_\perp$ value of Cu(A′) relative to that of Cu(A) is indicative of an increase in the in-plane Cu–O_z bond lengths, which is reasonable to expect as Cu^{2+} moves further into the β-cages from the plane of the six-ring window. That Cu^{2+} has moved into the β-cages on dehydration is evident from the weak interaction observed with adsorbed methanol. Methanol molecules are too bulky to enter the β-cage via the six-ring window. It is interesting to note that the ESR parameters in fully dehydrated Cu–CdX are similar to those in dehydrated Cu–NaX and different from those in dehydrated Cu–CaX. In previous studies[5] Cu^{2+} in dehydrated X and Y zeolites was suggested to be in SI and SI′ sites. However, rehydration of Cu–NaX does not result in formation of the trigonal-bipyramidal Cu(A) while it does in Cu–CdX. Thus we suggest that in dehydrated Cu–CdX, Cu^{2+} is most likely in SII′ sites so that it can move back into the SII sites on rehydration to form the trigonal-bipyramidal complex.

Conclusions

The ESR and ESEM studies on Cu^{2+} in fully cadmium exchanged X zeolites reveal the formation of an unusual trigonal-bipyramidal complex $Cu(O_z)_3(OH)_2$ which is observed in CaX zeolite and not in any other monovalent or divalent ion exchanged X zeolites. The stability of this complex in CdX was found to be less than than in CaX. However, unlike in CaX, this complex could be completely recovered on rehydration after dehydration of the zeolite at 500–700 K. Such regeneration seems to be due to the fact that Cu^{2+} is at different sites in the dehydrated Cu–CdX and Cu–CaX.

Acknowledgment. This research was supported by the National Science Foundation and the Robert A. Welch Foundation. We are grateful to the University of Houston Energy Laboratory for equipment support.

Registry No. Cu, 7440-50-8; Cd, 7440-43-9.

Coverage Dependence of Gas–Surface Energy Transfer

Daqing Zhao and John E. Adams*

Department of Chemistry, University of Missouri, Columbia, Missouri 65211

Received February 22, 1985. In Final Form: May 31, 1985

The energy transfer occurring when an energy-selected argon atom beam impinges on a tungsten(110) surface is examined via a classical trajectory simulation. Of special interest here is the enhancement of energy exchange observed when a submonolayer coverage of the argon test gas is adsorbed on and equilibrated with the metal surface. The computed scattering distributions are found to be in agreement with the limited experimental data available at present and are interpretable in terms of the adsorbate's effect on the surface roughness.

I. Introduction

The energy transfer accompanying the scattering of rare gases from metal surfaces has been the subject of numerous investigations, the earliest work coming shortly after the turn of the century. In these older studies the principal focus was on the determination of thermal accommodation coefficients, with the pioneering work of Roberts[1] and the subsequent results by Thomas and co-workers[2] constituting some of the more significant contributions to the field. Accommodation coefficients (hereafter, AC's) have been reported not only for gases in contact with clean metallic surfaces (although the presence of adsorbed atoms identical with those of the test gas could not be ruled out) but also for surfaces deliberately dosed with an adsorbate (for example, an alkali metal).[3] Some of the more recent work, however, has involved the use of techniques that permit a somewhat greater control over the experimental conditions. Both Yamamoto and Stickney[4] and also Weinberg and Merrill[5] have directed atomic beams at single-crystal W(110) surfaces and have determined angular distributions for the scattered rare gas atoms. Additional detail is revealed in the experiments of Janda, Hurst, and co-workers,[6,7] who reported time-of-flight distributions for a beam of argon atoms scattered from a polycrystalline tungsten or platinum(111) surface.[8]

The appearance of these experimental results for well-defined systems has sparked a renewed interest in theoretical studies of gas–surface energy transfer, with the contributions made to date ranging from the simple dy-

(1) Roberts, J. K. *Proc. R. Soc. London, Ser. A* **1930**, *129*, 146.
(2) See, for example: Thomas, L. B. In "Fundamentals of Gas-Surface Interactions"; Saltsburg, H., Smith, J. N., Jr., Eds.; Academic Press: New York, 1967; p 346.
(3) Thomas, L. B. In "Rarefied Gas Dynamics"; Fisher, S. S., Ed.; American Institute of Aeronautics and Astronautics: New York, 1981; p 83.
(4) Yamamoto, S.; Stickney, R. E. *J. Chem. Phys.* **1970**, *53*, 1594.
(5) Weinberg, W. H.; Merrill, R. P. *J. Chem. Phys.* **1972**, *56*, 2881.
(6) Janda, K. C.; Hurst, J. E.; Becker, C. A.; Cowin, J. P.; Auerbach, D. J.; Wharton, L. *J. Chem. Phys.* **1980**, *72*, 2403.
(7) Hurst, J. E.; Wharton, L.; Janda, K. C.; Auerbach, D. J. *J. Chem. Phys.* **1983**, *78*, 1559.
(8) For studies of inelastic scattering from insulator surfaces, see: Brusdeylins, G.; Doak, R. B.; Skofronick, J. G.; Toennies, J. P. *Surf. Sci.* **1983**, *128*, 191. Several groups recently have also addressed questions concerning the nature of inelastic molecule–surface scattering, with rotational state distributions and state-to-state rotational transition probabilities being reported for diatomics scattered from single-crystal surfaces. See, for example: Cowin, J. P.; Yu, C. F.; Sibener, S. J.; Hurst, J. E. *J. Chem. Phys.* **1981**, *75*, 1033. Cowin, J. P.; Yu, C. F.; Sibener, S. J.; Wharton, L. *J. Chem. Phys.* **1983**, *79*, 3537. Frenkel, F.; Häger, J.; Krieger, W.; Walther, H.; Campbell, C. T.; Ertl, G.; Kuipers, H.; Segner, J. *Phys. Rev. Lett.* **1981**, *46*, 152. McClelland, G. M.; Kubiak, G. D.; Rennagel, H. G.; Zare, R. N. *Phys. Rev. Lett.* **1981**, *46*, 831. Brusdeylins, G.; Toennies, J. P. *Surf. Sci.* **1983**, *126*, 647.

0743-7463/85/2401-0557$01.50/0